

## STRUCTURAL AND MAGNETIC PROPERTIES OF SINTERED (Nd, Tb)-(Fe, Ti)-(B, C) PERMANENT MAGNETS

STEFAN SZYMURA<sup>1,2\*</sup>, ALEKSANDER A. LUKIN<sup>3</sup>, HENRYK BALA<sup>4</sup>,  
ALEKSANDRA ŻURAWSKA<sup>1</sup>

The effect of different addition of carbon on the structural and magnetic properties of the sintered  $\text{Nd}_{14.60}\text{Tb}_{0.20}\text{Fe}_{\text{bal}}\text{Ti}_{1.24}\text{B}_{6.40}$  permanent magnet material are investigated by means of scanning electron microscopy (SEM), differential scanning calorimetry (DSC), Mössbauer spectroscopy (MS) and microhardness (HV). The results confirm that carbon increases the values ( $B_{\text{Hf}}$ ) of the hyperfine magnetic fields and the Curie temperature ( $T_{\text{C}}$ ) of the investigated permanent magnet material. The  $B_{\text{Hf}}$  parameters and the  $T_{\text{C}}$  for 0.12 wt.% C addition are the same as those observed for the permanent magnet material without Ti. An addition of 0.12 wt.% C improves the values of  $B_{\text{r}}$ ,  $(BH)_{\text{max}}$  and the corrosion resistance only slightly reducing the coercive force  $H_{\text{c}}$ . The influence of ageing temperature on the  $H_{\text{c}}$ , the microhardness (HV) and the Mössbauer parameters line width ( $G$ ) is also presented. It is suggested that the mechanism of the  $H_{\text{c}}$  changes during ageing is limited by relieving the internal stresses in the main phases and by changes of the microstructure in a nanoscale region.

Key words: intermetallic, microstructure, magnetic properties, microhardness, Mössbauer spectroscopy

### ŠTRUKTÚRNE A MAGNETICKÉ VLASTNOSTI SPEKANÝCH PERMANENTNÝCH MAGNETOV TYPU (Nd, Tb)-(Fe, Ti)-(B, C)

Článok sa zaoberá skúmaním vplyvu obsahu uhlíka na štruktúru a magnetické vlastnosti spekaných permanentných magnetov  $\text{Nd}_{14.60}\text{Tb}_{0.20}\text{Fe}_{\text{bal}}\text{Ti}_{1.24}\text{B}_{6.40}$ . Na hodno-

<sup>1</sup> Department of Physics, Technical University of Opole, 45-370 Opole, ul. Ozimska 75, Poland

<sup>2</sup> State Higher Vocational School in Nysa, 48-300 Nysa, Ul. Grodzka 19, Poland

<sup>3</sup> Centre of Magnetic Technologies, 117296 Moscow, Obrucheve Str. 52, Russia

<sup>4</sup> Department of Chemistry, Technical University of Częstochowa, 42-201 Częstochowa, Al. Armii Krajowej 19, Poland

\* corresponding author, e-mail: [szym@p1o.p1o.opole.pl](mailto:szym@p1o.p1o.opole.pl)

tenie sa použila metóda riadkovacej elektrónovej mikroskopie (SEM), diferenčnej skenovacej kalorimetrie (DSC), Mössbauerova spektroskopia (MS) a hodnotenie mikrotvrdosti (HV). Výsledky potvrdili, že uhlík v skúmaných vzorkách zvyšuje hodnoty hyperjemných magnetických polí ( $B_{\text{Hf}}$ ) a Curieho teplotu ( $T_C$ ). Hodnoty  $B_{\text{Hf}}$  a  $T_C$  pri obsahu 0,12 hm.% C sú totožné s hodnotami pre permanentné magnety bez obsahu Ti. Prídavok 0,12 hm.% C zlepšuje  $B_r$ ,  $(BH)_{\text{max}}$  a odolnosť voči korózii, pričom koercitívna sila  $H_c$  klesá len málo. Je tiež uvedený vplyv teploty starnutia na  $H_c$ , mikrotvrdosť (HV) a šírku čiar ( $G$ ) Mössbauerovho spektra. Predpokladá sa, že mechanizmus zmien  $H_c$  počas starnutia je limitovaný uvoľňovaním vnútorných napätí hlavných fáz a zmenami mikroštruktúry v nanooblastiach.

## 1. Introduction

It has been shown that many different elements can be substituted for the rare earth, iron or boron constituents of the  $R_2\text{Fe}_{14}\text{B}$  compound without alternating the 2 : 14 : 1 structure, which serves the purpose of improving some magnetic properties, thermal stability and corrosion resistance of the compound [1–3]. It has been found out that carbon only can be substituted for boron. The  $R_2\text{Fe}_{14}\text{C}$  compounds are characterized by a slightly lower Curie temperature and magnetization saturation; however, they display a higher level of magnetocrystalline anisotropy  $H_A$  [4]. It must be stressed that the  $R_2\text{Fe}_{14}\text{C}$  compounds are much more difficult to prepare than their  $R_2\text{Fe}_{14}\text{B}$  counterparts [2]. Moreover, the  $R_2\text{Fe}_{14}\text{C}$  compounds are in equilibrium with either ferromagnetic and/or very corrosive phases; therefore, the pure NdFeC material is useless here. This can be changed by an addition of several elements to the NdFeC materials. To improve magnetic properties and corrosion resistance by means of Nd-carbides, the investigation has been extended to higher order systems. Favourable phase relations with respect to corrosion have been observed in the quinary Nd-Fe-B-C cast alloy [5]. An addition of a correct amount of Cu leads to a new phase relation between the hard magnetic phase and  $\text{Nd}_x\text{Cu}_y$  compounds. The intermetallics created this way are non-magnetic and have a low melting point temperature.

Quite recently Lukin and Szymura [6] studied the effect of solid state reaction of the  $\text{Nd}_{14.60}\text{Tb}_{0.20}\text{Fe}_{\text{bal}}\text{Ti}_{1.24}\text{B}_{6.40}$  alloy with carbon. It has been confirmed that 0.12 wt.% C increases the remanence, the maximum energy product, the Curie temperature as well as the intrinsic corrosion, but it slightly reduces the intrinsic coercivity. This paper is in a way a continuation of the previous work [6] as it constitutes its vital accomplishment aiming at detecting the reasons for the change of the characteristics of the sintered  $\text{Nd}_{14.60}\text{Tb}_{0.20}\text{Fe}_{\text{bal}}\text{Ti}_{1.24}\text{B}_{6.40} + \text{C}_x$  ( $x = 0.06, 0.12, 0.16$  [wt.%]) permanent magnets.

## 2. Experimental details

Samples of nominal composition of  $\text{Nd}_{14.60}\text{Tb}_{0.20}\text{Fe}_{\text{bal}}\text{Ti}_{1.24}\text{B}_{6.40}$  were prepared by means of conventional argon arc-melting of the constituents characterized

by purity  $\geq 99.9\%$ . Ingots were sealed in an evacuated quartz tube protected with Mo foil and annealed at 1473 K for seven days. In the  $\text{Nd}_{14.60}\text{Tb}_{0.20}\text{Fe}_{\text{bal}}\text{Ti}_{1.24}\text{B}_{6.40}$  alloy, the oxygen, nitrogen, hydrogen and carbon concentrations were 110 ppm, 65 ppm, 12 ppm and 0.03 wt.%, respectively. The alloy powder was prepared by means of ball milling of the  $\text{Nd}_{14.60}\text{Tb}_{0.20}\text{Fe}_{\text{bal}}\text{Ti}_{1.24}\text{B}_{6.40}$  ingots; this in turn was kept in gasoline for protection against oxidation. The  $\text{Nd}_{14.60}\text{Tb}_{0.20}\text{Fe}_{\text{bal}}\text{Ti}_{1.24}\text{B}_{6.40}$  powder particles were from 2 to 5  $\mu\text{m}$  in diameter. Then the  $\text{Nd}_{14.60}\text{Tb}_{0.20}\text{Fe}_{\text{bal}}\text{Ti}_{1.24}\text{B}_{6.40}$  alloy and powdered carbon (99.998% of purity, powder size less than 1  $\mu\text{m}$ ) in various concentrations (0.06, 0.12, 0.16 wt.%) were mechanically mixed and pressed into the cube shape under the pressure of 0.1 GPa in the magnetic field of 1.5 T transverse to the pressing direction, and sintered at 1373 K in a vacuum furnace at the pressure level of  $4 \times 10^{-3}$  Pa for 2 hours, and then rapidly cooled to the room temperature within 3 minutes. Since all the alloy powders had been dried in a vacuum chamber, the amount of the residual carbon in the sintered magnets (without C additional powders) after gasoline coating was determined to be very low (about 0.08 wt.%), which was typical of a technological process. The samples were isothermally annealed at different temperatures ranging from 600 to 1200 K for 1 hour in pure Ar atmosphere. Identical cooling conditions were applied in the case of different samples so as to avoid a relative variation of properties.

The densities of the tested permanent magnet samples, determined by means of comparison of their weight in air and in toluene, were the same within the limits of error set for the experimental method, and they equalled  $7.50 \pm 0.06$  g/cm<sup>3</sup>. The magnetic properties were estimated on the basis of demagnetization curves measured with a hysteresis graph with the maximum magnetic field of 2.4 MA/m. The Curie temperature ( $T_C$ ) of permanent magnet samples was determined with the accuracy of  $\pm 0.5$  K by specific heat measurements conducted by means of the Perkin-Elmer Differential Scanning Calorimeter.

Phases present in the annealed samples were studied by means of electron microscope scanning (SEM) and energy dispersive X-ray spectroscopy (EDAX). The measurements of microhardness (HV) were carried out with the "Leitz" microhardness test at: the grain matrix phase ( $\text{HV}_\Phi$ ), the grain junction ( $\text{HV}_g$ ) and the corners ( $\text{HV}_c$ ). All the observations (SEM) and examinations (EDAX and HV) of thermally demagnetized permanent magnet samples were performed on a polished surface located perpendicularly to the alignment direction (ease axis). The <sup>57</sup>Fe Mössbauer spectra were recorded at room temperature by means of the constant acceleration Mössbauer spectrometer in the transmission mode with the 0.5 GBq <sup>57</sup>Co (Cr) source. The Mössbauer spectrometer was calibrated with the  $\alpha$ -iron foil 20  $\mu\text{m}$  thick.

### 3. Results and discussion

It is well known, that while the correct chemical composition of the NdFeB type permanent magnets is vital for obtaining the optimal magnetic properties,

their microstructure is important in determining their intrinsic coercivity and remanence [7], the corrosion resistance [8] and mechanical properties [9]. However, various factors control the structure and chemical composition of individual phases. Among these factors the post-sintering heat treatment is most important, especially for the intrinsic coercivity. The sintered  $\text{Nd}_{14.60}\text{Tb}_{0.20}\text{Fe}_{\text{bal}}\text{Ti}_{1.24}\text{B}_{6.40} + \text{C}$  permanent magnet samples ageing for 1 hour reach the minimum and maximum of intrinsic coercivity ( $iH_c^{\text{min}} = 520 \text{ kA/m}$  and  $iH_c^{\text{max}} = 1080 \text{ kA/m}$ ) at respective temperatures of 725 K and 1025 K, which confirms our earlier expectations [10].

The microhardness test of a permanent magnet sample, for instance  $\text{Nd}_{14.60}\text{Tb}_{0.20}\text{Fe}_{\text{bal}}\text{Ti}_{1.24}\text{B}_{6.40} + 0.12 \text{ wt.}\% \text{ C}$ , after the ageing leading to  $iH_c^{\text{min}}$  and  $iH_c^{\text{max}}$  have shown that for the low coercive condition in the central part of the  $\Phi$ -phase grains, it is homogenous and exhibits the values of  $800 \pm 40$ . However, on the grain junction ( $\text{HV}_g$ ) and on the corners ( $\text{HV}_c$ ) the microhardness is considerably smaller; in relative units to the grain centre, the  $\text{HV}_g$  and  $\text{HV}_c$  were 0.72–0.89 and 0.75–0.95, respectively. In the permanent magnet samples with  $iH_c^{\text{max}}$  the situation is different, i.e. the microhardness becomes fairly similar for  $\text{HV}_g$  (0.77–0.85) and for  $\text{HV}_c$  (0.74–0.95) by contrast to the microhardness of  $\text{HV}_\Phi$  (0.75–0.93). This seems to be connected with the stress relieving between the phases of the permanent magnet occurring while ageing.

The effects of the addition of C on the magnetic properties ( $B_r$ ,  $iH_c$  and  $(BH)_{\text{max}}$ ) and the Curie temperature ( $T_C$ ) of the sintered  $\text{Nd}_{14.60}\text{Tb}_{0.20}\text{Fe}_{\text{bal}}\text{Ti}_{1.24}\text{B}_{6.40} + \text{C}_x$  ( $x = 0, 0.06, 0.12, 0.16 \text{ wt.}\%$ ) annealed at 1025 K for 1 hour are listed in Table 1. It can be seen that the properties of the tested permanent magnets change significantly if carbon powder is introduced to the  $\text{Nd}_{14.60}\text{Tb}_{0.20}\text{Fe}_{\text{bal}}\text{Ti}_{1.24}\text{B}_{6.40}$  alloy. The increase of remanence ( $B_r$ ) of the maximum value of 1.31 T is achieved in the permanent magnet sample with the addition of 0.12 wt.% C. An analogous dependence is observed for maximum energy product  $(BH)_{\text{max}}$  and the Curie temperature ( $T_C$ );  $T_C$  increases to  $583 \pm 0.5 \text{ K}$ , which corresponds to the value of  $T_C$  for a permanent magnet without an addition of Ti. However, the intrinsic coercivity ( $iH_c$ ) slowly decreases along with the increase of the content of C.

The grain size of the hard magnetic  $\text{Nd}_2\text{Fe}_{14}\text{B}$  phase and the relative position of the non-magnetic phase versus the magnetic one have a crucial significance in determining the hard magnetic properties of the sintered NdFeB type of permanent magnets. Fairly recently, Pan et al. [11] have reported the experimental results of the solid state reaction of the  $\text{Nd}_2\text{Fe}_{14}\text{B}$  with carbon and discussed the phase evolution. The experimental results have revealed that the phase evolution of  $\text{Nd}_{12}\text{Fe}_{14}\text{B} + \text{C}$  is highly sensitive to the carbon concentration and the sintering temperature. Of the  $\text{NdFeB} + 0.2 \text{ wt.}\% \text{ C}$  samples sintered at temperatures ranging from 923 to 1373 K, the main phase of the permanent magnets sintered at all temperatures is the  $\text{Nd}_2\text{Fe}_{14}\text{B}$  phase.

Table 1. Magnetic properties and the Curie temperature of the sintered  $\text{Nd}_{1.4.60}\text{Tb}_{0.20}\text{Fe}_{\text{bal}}\text{B}_{6.40}$  and the  $\text{Nd}_{1.4.60}\text{Tb}_{0.20}\text{Fe}_{\text{bal}}\text{Ti}_{1.24}\text{B}_{6.40} + C_x$  ( $x = 0, 0.06, 0.12, 0.16$  wt.%) permanent magnets

No.	Permanent magnet material	Remanence $B_r$ [T]	Intrinsic coercivity $iH_c$ [kA/m]	Maximum energy product $(BH)_{\text{max}}$ [kJ/m <sup>3</sup> ]	Curie temperature $T_C$ [K]
1.	$\text{Nd}_{1.4.60}\text{Tb}_{0.20}\text{Fe}_{\text{bal}}\text{B}_{6.40}$	1.32	980	319	582.0
2.	$\text{Nd}_{1.4.60}\text{Tb}_{0.20}\text{Fe}_{\text{bal}}\text{Ti}_{1.24}\text{B}_{6.40}$	1.25	1080	294	561.0
3.	$\text{Nd}_{1.4.60}\text{Tb}_{0.20}\text{Fe}_{\text{bal}}\text{Ti}_{1.24}\text{B}_{6.40} + 0.06$ wt.% C	1.29	1015	314	574.0
4.	$\text{Nd}_{1.4.60}\text{Tb}_{0.20}\text{Fe}_{\text{bal}}\text{Ti}_{1.24}\text{B}_{6.40} + 0.12$ wt.% C	1.31	970	320	583.0

Table 3. Mössbauer effect parameter such as the line width ( $G$ ) for the sintered  $\text{Nd}_{1.4.60}\text{Tb}_{0.20}\text{Fe}_{\text{bal}}\text{Ti}_{1.24}\text{B}_{6.40} + 0.12$  wt.% C permanent magnets with the minimum and maximum values of the intrinsic coercivity ( $iH_c$ )

Mössbauer parameters	Permanent magnet materials	Fe atom sites					
		16k <sub>1</sub>	16k <sub>2</sub>	8j <sub>1</sub>	8j <sub>2</sub>	4e	4c
The magnetic hyperfine field $B_{\text{HF}}$ [T]	$\text{Nd}_{1.4.60}\text{Tb}_{0.20}\text{Fe}_{\text{bal}}\text{B}_{6.40}$	28.9 ± 0.1	30.6 ± 0.1	26.1 ± 0.2	34.4 ± 0.2	31.1 ± 0.3	25.1 ± 0.3
	$\text{Nd}_{1.4.60}\text{Tb}_{0.20}\text{Fe}_{\text{bal}}\text{Ti}_{1.24}\text{B}_{6.40}$	28.1 ± 0.1	30.2 ± 0.1	25.4 ± 0.2	34.4 ± 0.2	30.6 ± 0.3	24.5 ± 0.3
	$\text{Nd}_{1.4.60}\text{Tb}_{0.20}\text{Fe}_{\text{bal}}\text{Ti}_{1.24}\text{B}_{6.40} + 0.06$ wt.% C	28.4 ± 0.1	30.3 ± 0.1	25.7 ± 0.2	34.5 ± 0.2	30.7 ± 0.3	25.7 ± 0.3
	$\text{Nd}_{1.4.60}\text{Tb}_{0.20}\text{Fe}_{\text{bal}}\text{Ti}_{1.24}\text{B}_{6.40} + 0.12$ wt.% C	28.8 ± 0.1	30.6 ± 0.1	26.0 ± 0.2	34.4 ± 0.2	31.1 ± 0.3	25.2 ± 0.3
The isomer shift $\delta$ [mm/s]	$\text{Nd}_{1.4.60}\text{Tb}_{0.20}\text{Fe}_{\text{bal}}\text{B}_{6.40}$	-0.07 ± 0.01	-0.11 ± 0.01	-0.05 ± 0.02	0.08 ± 0.02	-0.04 ± 0.04	-0.16 ± 0.04
	$\text{Nd}_{1.4.60}\text{Tb}_{0.20}\text{Fe}_{\text{bal}}\text{Ti}_{1.24}\text{B}_{6.40}$	-0.07 ± 0.01	-0.10 ± 0.01	-0.05 ± 0.02	0.09 ± 0.02	-0.05 ± 0.04	-0.17 ± 0.04
	$\text{Nd}_{1.4.60}\text{Tb}_{0.20}\text{Fe}_{\text{bal}}\text{Ti}_{1.24}\text{B}_{6.40} + 0.06$ wt.% C	-0.07 ± 0.01	-0.10 ± 0.01	-0.07 ± 0.02	0.09 ± 0.02	-0.06 ± 0.04	-0.15 ± 0.04
	$\text{Nd}_{1.4.60}\text{Tb}_{0.20}\text{Fe}_{\text{bal}}\text{Ti}_{1.24}\text{B}_{6.40} + 0.12$ wt.% C	-0.07 ± 0.01	-0.11 ± 0.01	-0.05 ± 0.02	0.08 ± 0.02	-0.04 ± 0.04	-0.16 ± 0.04
The quadrupole shift $2\epsilon$ [mm/s]	$\text{Nd}_{1.4.60}\text{Tb}_{0.20}\text{Fe}_{\text{bal}}\text{B}_{6.40}$	0.21 ± 0.02	0.11 ± 0.02	0.07 ± 0.04	0.64 ± 0.04	0.11 ± 0.06	-0.17 ± 0.06
	$\text{Nd}_{1.4.60}\text{Tb}_{0.20}\text{Fe}_{\text{bal}}\text{Ti}_{1.24}\text{B}_{6.40}$	0.22 ± 0.02	0.13 ± 0.02	0.09 ± 0.04	0.64 ± 0.04	0.12 ± 0.06	-0.14 ± 0.06
	$\text{Nd}_{1.4.60}\text{Tb}_{0.20}\text{Fe}_{\text{bal}}\text{Ti}_{1.24}\text{B}_{6.40} + 0.06$ wt.% C	0.23 ± 0.02	0.12 ± 0.02	0.08 ± 0.04	0.63 ± 0.04	0.11 ± 0.06	-0.18 ± 0.06
	$\text{Nd}_{1.4.60}\text{Tb}_{0.20}\text{Fe}_{\text{bal}}\text{Ti}_{1.24}\text{B}_{6.40} + 0.12$ wt.% C	0.21 ± 0.02	0.11 ± 0.02	0.07 ± 0.04	0.64 ± 0.04	0.11 ± 0.06	-0.17 ± 0.06

Figure 1, as an example, gives representative SEM micrographs with the atomic number contrast enhanced by backscattered imaging, the  $\text{Nd}_{14.60}\text{Tb}_{0.20}\text{Fe}_{\text{bal}}\text{Ti}_{1.24}\text{B}_{6.40}$  (Figs. 1a and 1b) and the  $\text{Nd}_{14.60}\text{Tb}_{0.20}\text{Fe}_{\text{bal}}\text{Ti}_{1.24}\text{B}_{6.40} + 0.12 \text{ wt.}\% \text{ C}$  (Fig. 1c), sintered at 1373 K for 2 hours, in the  $iH_c^{\text{max}}$  state. The microstructure and grain size of less than  $20 \mu\text{m}$  of the tested permanent magnet samples is comparable to sintered materials. The sintered  $\text{Nd}_{14.60}\text{Tb}_{0.20}\text{Fe}_{\text{bal}}\text{Ti}_{1.24}\text{B}_{6.40}$  permanent magnet consists of four phases, i.e. the  $\text{Nd}_2\text{Fe}_{14}\text{B}$  hard magnetic phase ( $\Phi$ -phase), the Nd-rich phase (n-phase), the  $\text{TiB}_2$ -phase and, of the smallest amount, the  $\text{Nd}_{1.1}\text{Fe}_4\text{B}_4$ -phase ( $\eta$ -phase) marked by A, B, T and C in Fig. 1a, respectively. After the 0.12 wt.% C addition to a permanent magnet (Fig. 1c) one additional

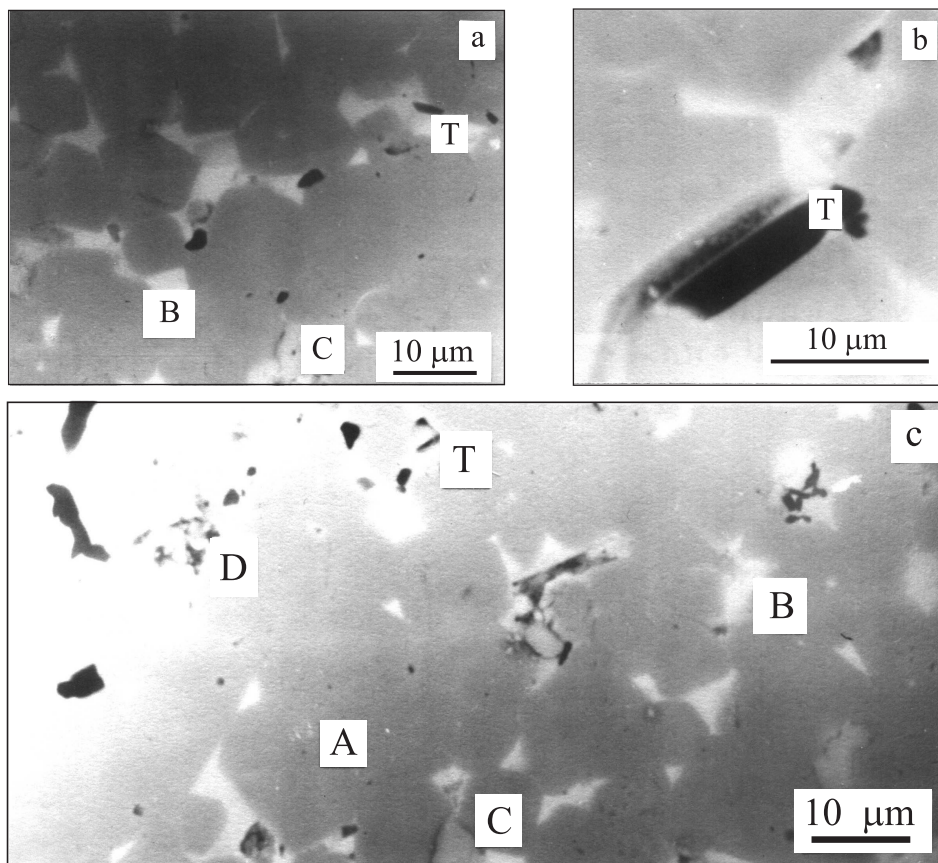


Fig. 1. Backscattered electron SEM micrographs of the sintered  $\text{Nd}_{14.60}\text{Tb}_{0.20}\text{Fe}_{\text{bal}}\text{Ti}_{1.24}\text{B}_{6.40}$  (a, b) and the  $\text{Nd}_{14.60}\text{Tb}_{0.20}\text{Fe}_{\text{bal}}\text{Ti}_{1.24}\text{B}_{6.40} + 0.12 \text{ wt.}\% \text{ C}$  (c) permanent magnets. Different observed areas are summarized in the text.

phase (marked as D in Fig. 1c) is observed mainly along the grain boundaries between the grains of the hard magnetic  $\Phi$ -phase which have the approximate composition (in wt.%): 2.9 Nd, 4 Fe, 6.7 Ti, 11 B, 15.2 C. These phases and  $\text{TiB}_2$ -phases decouple the magnetically hard  $\Phi$  grains and exhibit a very good corrosion resistance. The measurements of corrosion in maritime environment show an improvement by an approximate factor at the level of two [6].

The matrix  $\text{Nd}_2\text{Fe}_{14}\text{B}$  phase for the sintered  $\text{Nd}_{14.60}\text{Tb}_{0.20}\text{Fe}_{\text{bal}}\text{Ti}_{1.24}\text{B}_{6.40}$  permanent magnet samples in the  ${}_iH_c^{\text{max}}$  state contains 0.45 wt.% Ti. The Ti content in this phase decreases with the increase of the amount of C in the permanent magnet samples; for the 0.12 wt.% C addition, the  $\Phi$ -phase has a concentration of Ti approaching zero. On the other hand, the  $\Phi$ -phase does not display any detectable amount of C.

In Table 2 we report the fitted hyperfine parameters of the  $\text{Nd}_2\text{Fe}_{14}\text{B}$  phase contribution to the Mössbauer spectra of the sintered  $\text{Nd}_{14.60}\text{Tb}_{0.20}\text{Fe}_{\text{bal}}\text{Ti}_{1.24}\text{B}_{6.40} + \text{C}_x$  ( $x = 0, 0.06$  and  $0.12$  wt.%) permanent magnet samples, for the purpose of comparison to the sintered  $\text{Nd}_{14.60}\text{Tb}_{0.20}\text{Fe}_{\text{bal}}\text{Ti}_{1.24}\text{B}_{6.40}$  permanent magnet. The Mössbauer absorption spectra consist of sextets corresponding with six different crystal sites occupied by the Fe atom. For a given site the value of the isomer shift, the quadrupole shift and hyperfine magnetic fields symbolized respectively by  $\delta$ ,  $2\varepsilon$  and  $B_{\text{Hf}}$ , are reported in Table 2. For a given site the values of  $\delta$  and  $2\varepsilon$  are similar, the experimental error taken into consideration, while the values of  $B_{\text{Hf}}$  are different. The  $B_{\text{Hf}}$  values, except for  $8j_2$  site, increase with C concentration in all the Fe sites and for 0.12 wt.% C they are practically equal to the values for the permanent magnet without Ti. Additionally, in Table 3 we report the value of the line width  $G$  for the sintered  $\text{Nd}_{14.60}\text{Tb}_{0.20}\text{Fe}_{\text{bal}}\text{Ti}_{1.24}\text{B}_{6.40} + 0.12$  wt.% C permanent magnet samples in  ${}_iH_c^{\text{min}}$  and  ${}_iH_c^{\text{max}}$  state. It can be seen that a higher

Table 2. Hyperfine parameters of the  $\text{Nd}_2\text{Fe}_{14}\text{B}$  contribution in  $\text{Nd}_{14.60}\text{Tb}_{0.20}\text{Fe}_{\text{bal}}\text{B}_{6.40}$  and the  $\text{Nd}_{14.60}\text{Tb}_{0.20}\text{Fe}_{\text{bal}}\text{Ti}_{1.24}\text{B}_{6.40} + \text{C}_x$  ( $x = 0, 0.06, 0.12$  wt.%) permanent magnets

Intrinsic coercivity ${}_iH_c$ [kA/m]	520	1080
The line width $G$ [m/s]		
Fe atom sites		
16k <sub>1</sub>	0.365	0.402
16k <sub>2</sub>	0.362	0.400
8j <sub>1</sub>	0.370	0.397
8j <sub>2</sub>	0.348	0.382
4e	0.369	0.400
4c	0.362	0.391

value of  $iH_c$  of a permanent magnet sample corresponds to a higher value of the line width. This seems to be connected with stress relieving internally the main phases of the permanent magnet which takes place during the process of annealing. Thus, it should be assumed that the observed changes of HV do not result from the formation of mechanical stress during ageing [12, 13], but rather they concern the changes of the microstructure in the nano-scale region [10, 14].

#### 4. Conclusions

The  $\text{Nd}_{14.60}\text{Tb}_{0.20}\text{Fe}_{\text{bal}}\text{Ti}_{1.24}\text{B}_{6.40}$  alloys were prepared by the induction melting technique. Carbon was introduced into the alloys upon a solid state reaction (sintering at 1373 K for 2 hours). The addition of 0.12 wt.% C substantially increased the remanence and maximum energy product, as well as the Curie temperature, along with a slight decrease of the intrinsic coercivity. The corrosion resistance was also improved, which might be due to the reduction of the content of Ti in the hard magnetic phase practically to the zero level, and to the formation of non-magnetic grain boundary phases without forming non-magnetic grains. Therefore, high performance and corrosion resistive permanent magnet materials may be developed by the combining of small additions of Ti and C to (Nd, Tb)FeB alloys.

#### REFERENCES

- [1] HERBST, J. F.: *Rev. Mod. Phys.*, **63**, 1991, p. 819.
- [2] BUSCHOW, K. H. J.: *Rep. Prog. Phys.*, **54**, 1991, p. 1123.
- [3] MORRISH, A. H.—LI, Z. W.—ZHOU, X. Z.—DAI, S.: *J. Phys. D: Appl. Phys.*, **29**, 1996, p. 2290.
- [4] GRÖSSINGER, R.—KREWENKA, R.—KOU, X. C.—BUSCHOW, K. H. J.: *J. Magn. Magn. Mater.*, **83**, 1990, p. 130.
- [5] GRIEB, B.—FRITZ, K.—HENIG, E. Th.: *J. Appl. Phys.*, **70**, 1991, p. 6359.
- [6] LUKIN, A. A.—SZYMURA, S.: *Intermetallics*, **9**, 2001, p. 169.
- [7] KRONMÜLLER, H.—DURST, K. H.—HOCK, K. D.—MARTINEK, G.: *J. Phys. (Paris)*, **490**, 1988, p. C8-623.
- [8] BALA, H.—SZYMURA, S.—PAWŁOWSKA, G.—RABINOVICH, Yu. M.: *Arch. Mater. Sci.*, **49**, 1996, p. 225.
- [9] RABINOVICH, Yu. M.—SERGEEV, V. V.—MAYSTRENKO, A. D.—KULAKOWSKI, V.—SZYMURA, S.—BALA, H.: *Intermetallics*, **4**, 1996, p. 641.
- [10] SZYMURA, S.—LUKIN, A. A.—ZHURAVLYEV, A. A.—MARGARYAN, M. C.—RABINOVICH, Yu. M.—BALA, H.: *Phys. Stat. Sol. (a)*, **174**, 1999, p. 513.
- [11] PAN, F.—ZHANG, M.—ZHAO, R. F.—LIU, B. X.—TOKUNAGA, M.: *J. Phys. D: Appl. Phys.*, **31**, 1998, p. 488.
- [12] STADELMAIER, H. H.—STRNAT, K. J.: In: *Proc. 10<sup>th</sup> Worksh. Rare-Earth Magnets and their Appl.* Ed.: Shinjo, M. Tokyo, The Society of Non-Traditional Technology 1989, p. 53.



- 
- [13] WHITNEY, P. A.—DEVLIN, E. J.—ABELL, J. S.—HARRIS, I. R.: *J. Magn. Magn. Mater.*, 80, 1993, p. 2755.
- [14] LUKIN, A. A.—SZYMURA, S.—ZHURAVLYEV, A. A.—NOWY-WIECHUA, W.: *Modern Phys. Lett. B*, 13, 1999, p. 681.

Recived: 3.5.2004